

FINAL REPORT

Helicopter Magnetometer Platform based on Compact Induction Sensors

SERDP Project MM-1594

DECEMBER 2007

Dr. Yongming Zhang
QUASAR Federal Systems, Inc.

This document has been approved for public release.



Strategic Environmental Research and
Development Program

Report Documentation Page				Form Approved OMB No. 0704-0188	
Public reporting burden for the collection of information is estimated to average 1 hour per response, including the time for reviewing instructions, searching existing data sources, gathering and maintaining the data needed, and completing and reviewing the collection of information. Send comments regarding this burden estimate or any other aspect of this collection of information, including suggestions for reducing this burden, to Washington Headquarters Services, Directorate for Information Operations and Reports, 1215 Jefferson Davis Highway, Suite 1204, Arlington VA 22202-4302. Respondents should be aware that notwithstanding any other provision of law, no person shall be subject to a penalty for failing to comply with a collection of information if it does not display a currently valid OMB control number.					
1. REPORT DATE 01 DEC 2007		2. REPORT TYPE N/A		3. DATES COVERED -	
4. TITLE AND SUBTITLE Helicopter Magnetometer Platform based on Compact Induction Sensors				5a. CONTRACT NUMBER	
				5b. GRANT NUMBER	
				5c. PROGRAM ELEMENT NUMBER	
6. AUTHOR(S)				5d. PROJECT NUMBER	
				5e. TASK NUMBER	
				5f. WORK UNIT NUMBER	
7. PERFORMING ORGANIZATION NAME(S) AND ADDRESS(ES) QUASAR Federal Systems, Inc.				8. PERFORMING ORGANIZATION REPORT NUMBER	
9. SPONSORING/MONITORING AGENCY NAME(S) AND ADDRESS(ES)				10. SPONSOR/MONITOR'S ACRONYM(S)	
				11. SPONSOR/MONITOR'S REPORT NUMBER(S)	
12. DISTRIBUTION/AVAILABILITY STATEMENT Approved for public release, distribution unlimited					
13. SUPPLEMENTARY NOTES The original document contains color images.					
14. ABSTRACT					
15. SUBJECT TERMS					
16. SECURITY CLASSIFICATION OF:			17. LIMITATION OF ABSTRACT UU	18. NUMBER OF PAGES 29	19a. NAME OF RESPONSIBLE PERSON
a. REPORT unclassified	b. ABSTRACT unclassified	c. THIS PAGE unclassified			

This report was prepared under contract to the Department of Defense Strategic Environmental Research and Development Program (SERDP). The publication of this report does not indicate endorsement by the Department of Defense, nor should the contents be construed as reflecting the official policy or position of the Department of Defense. Reference herein to any specific commercial product, process, or service by trade name, trademark, manufacturer, or otherwise, does not necessarily constitute or imply its endorsement, recommendation, or favoring by the Department of Defense.

Helicopter Magnetometer Platform based on Compact Induction Sensors

(SERDP SEED Project 1594:2006)

Final Report

Dec 12th, 2007



Name	Address	Phone	E-Mail	POC Type
<u>Dr. Yongming Zhang</u>	QUASAR Federal Systems, Inc. 5754 Pacific Center Boulevard, Suite 203 San Diego, CA 92121	858-200-2229	yongming@quasarfs.com	LEAD PI

Project Summary

In this SERDP SEED project, QUASAR Federal Systems (QFS) carried out a proof-of-concept study for airborne UXO detection using AC induction sensor (IS) magnetometers. Current airborne UXO detection is dominated by Cs-vapor, DC total field magnetometers. These DC magnetometers are expensive, consume high power, and do not provide enough information about the shape or orientation of the target. QFS has recently developed a compact IS magnetometer with equivalent sensitivity to current state-of-the-art induction sensors in a significantly smaller package. The IS is an AC sensor which is insensitive to DC and near-DC noise and can provide vector magnetic information for targets.

QFS built a 3-axis induction sensor (6" long, 0.440" in diameter, 1.8 oz in weight for each axis), including a "main" tri-axial sensor, and a single axis reference sensor, which all had a noise floor of $20 \text{ pT}/\sqrt{\text{Hz}}$ @ 1 Hz. These sensors were optimized for the band of 0.5 - 15 Hz and used in several pre-flight experiments to quantify the signal strengths and frequency bands of both target and motion-induced signals. It was found that the motion-induced noise in the main sensor was reduced by about 10 dB when the sensor was aligned to the Earth's magnetic field.

Collaborating with Sky Research, the sensors were then deployed to the proposed flight tests. The main sensor was mounted in the center of the boom and the reference sensor was mounted in the far right side of the boom. The measured noise floor during these tests was 500x higher than the sensor noise floor, $\sim 10 \text{ nT}/\sqrt{\text{Hz}}$ @ 1 Hz. The post processed data gave an in-flight noise floor of $\sim 3 \text{ nT}/\sqrt{\text{Hz}}$ @ 1 Hz and was able to achieve an SNR ~ 13 for the largest target (100 lb bomb). During the flight tests, the reference sensor was not rigidly mounted to the main sensor. Thus the reference sensor was largely incoherent with the main sensor and did not provide effective cancellation. However some cancellation of motion-induced noise was possible with data from the off-axis sensor data in the 3-axis assembly, which were coherent with the main sensor.

Following the flight tests it became clear that the reference sensor should be mounted directly above the main sensor in a gradiometer configuration to maximize noise mitigation. Post-flight experiments were carried out to compare a lash-up induction sensor gradiometer to the original induction sensor magnetometer. The gradiometer, aligned to the Earth's field, showed a factor of 10x lower noise than the induction sensor. *We conclude that a noise floor of $1 \text{ nT}/\sqrt{\text{Hz}}$ @ 1 Hz is possible to achieve during flight.*

It is likely that the sensitivity of an induction sensor gradiometer could be pushed further. A more carefully constructed gradiometer would have a higher degree of coherence than the lash-up prototype used here. A 3-axis gradiometer and a rotation sensor, such as a gyroscope, would allow more cancellation of motion-induced noise. *It may be possible to achieve an in-flight noise floor of $\sim 100 \text{ pT}/\sqrt{\text{Hz}}$ @ 1 Hz; a factor of 10 lower than the noise floor achieved with Cs-vapor magnetometers.* In the end, a 3-axis gradiometer would have better sensitivity than current Cs-vapor magnetometers, would have no flight envelope restrictions, would be packaged to be smaller and lighter, and would provide vector information for target discrimination.

1. Introduction

Buried UXO disturbs the local magnetic field of the Earth, producing a characteristic magnetic signature that can be detected by a magnetometer. Sensors currently used for digital geophysical mapping of munitions sites are dominated by Cs-vapor magnetometers operating in the passive mode. A new type of magnetic induction sensor developed at QUASAR Federal Systems has the sensitivity and dynamic range of earlier technology, but is the same linear dimension and one-tenth the weight. These advances have made possible the first 3-axis orthogonal induction sensor module. The sensitivity of the sensor module (10 - 20 pT/rHz at 1 Hz) was verified by a field test in Oct. 2003 at the Nevada Test Site. *By using three orthogonal sensors, one can detect signatures from a buried UXO target in all three directions*, and therefore acquire information on the distance and direction of magnetic sources.

In recent years, a Helicopter-based Magnetometer Mapping System was developed by the Naval Research Lab and further modified by Sky Research. This Helicopter Magnetometer (Helimag) system consists of a Kevlar boom mounted on a Bell 206L or MD 530F helicopter. The boom has an array of 7 Cs-vapor, total-field magnetometers mounted along an axis perpendicular to the centerline of the helicopter. This system provides highly efficient digital mapping at survey rates of approximately 300-500 acres per day, with detection capability approaching that of ground-based methods¹. The sensor boom is mounted forward of the helicopter to minimize interference from the aircraft rotor, engine and avionics, is semi-rigid, and *has low-vibration characteristics*. This design puts the boom in clear view of the pilot to allow for safe, precise low-level flying. The magnetometers, spaced on the boom at 1.5 m intervals, allow survey speeds up to 30 m/s. The nominal survey altitude is 1.5 m to 3 m above ground level (AGL).

QFS proposed mounting a three-axis IS module and a reference sensor on Sky Research's Helimag Sensor Platform to detect magnetic field distortion generated by an UXO object buried in the ground. The moving platform would convert the DC magnetic signature into an AC signature with frequency components determined by the target size and orientation, as well as the speed and the flight height of the moving platform. The main advantages of this magnetic sensing technology are as follows:

- rejection of DC noise
- lower noise than Cs-magnetometer in the detection band
- better discrimination capability due to 3-axis vector signature
- lower cost, lighter weight, and much less power is required

2. Phase I Technical Objectives

The goal of this program was to study the feasibility of improving the Helicopter-based magnetometry technology by integrating a QFS 6"-long induction sensor onto Sky Research's low-noise, helicopter sensor platform. The 3-axis induction sensor was operated in the passive mode on the platform, which flew at $v = 5 - 30$ m/s and $h = 1.5$ and 3 m, in order to collect magnetic signatures from UXO targets buried in the ground. A 3-axis vector sensor provides more target discrimination information than a total field

magnetometer. Based on the fact that the sensor has a noise floor of 10 pT in the band of 0.5 Hz to 50 Hz, it was hoped that the platform could achieve a detection sensitivity of 20 - 100 pT in the band. In addition, QFS proposed to test a simple noise cancellation algorithm with a reference sensor mounted on the same platform.

3. Summary of Work Performed

The SEED project has been an extraordinary learning experience and good technical success was achieved on all tasks. Good collaboration has been achieved between the QFS team and Sky's team during the project.

While the sensor noise floor is $\sim 20 \text{ pT}/\sqrt{\text{Hz}}$ @ 1 Hz, the limiting factor of UXO detection is motion-induced noise due to the rotation of the induction sensor in the Earth's DC magnetic field. A considerable effort went into understanding and eliminating sources of noise in the system. In addition to the proposed flight tests, several pre-flight measurements and one post-flight measurement were carried out. These measurements were designed to test the capability of the moving sensors, identify sources of noise, mitigate the source, and characterize target signals. In summary, the work done during the SEED project was:

- A 3-axis sensor assembly was built, with the vertical axis acting as the “main” sensor. A single-axis reference sensor was also built. These sensors were a modification of an existing QFS design. The pass band and gain of the sensors was optimized for the application, with a noise floor of $20 \text{ pT}/\sqrt{\text{Hz}}$ @ 1 Hz.
- Motion Track Tests - a 3-m motion track was constructed. The track system allowed the sensors to be moved at constant velocity in the presence of targets. The induced noise was not so high as to saturate the sensors, and target detection was possible. It was found that aligning the main sensor to the Earth's magnetic field resulted in a significant reduction in motion-induced noise.
- Vehicle Tests - The sensors were mounted on a ground vehicle to carry out longer distance motion experiments. In the vehicle tests the sensors were again able to operate without saturating; UXO target detection was again possible, and the reference sensor showed some capability to cancel coherent noise.
- Flight Tests – The proposed flight tests were carried out at the Sky Research facility in Ashland, OR. Again the sensors functioned without saturating and detection of the largest target was successful. The dominant sources, frequencies, and signal strengths of flight-based noise were identified. The smaller targets were difficult to resolve and the reference sensor proved less useful at cancelling the motion noise from the helicopter. Some noise cancellation was possible using the off-axis sensors in the 3-axis assembly.
- Vehicle Based Gradiometer Tests – The primary lesson of the flight test was the need to cancel motion-induced noise in the magnetometers; primarily from the rotation of the vector sensor in the Earth's magnetic field. The induction sensors were configured as a gradiometer and the vehicle tests were repeated. It was found that a lash-up gradiometer, aligned to the Earth's field, could achieve a 50x reduction in motional noise over a vertical induction sensor. Target detection was significantly improved and an in-flight noise performance of $< 1 \text{ nT}/\sqrt{\text{Hz}}$ @ 1 Hz seems possible.

4. Detailed Description of Project Activities

The program was divided into 3 principle tasks. The specific goals for each task are copied verbatim from the SEED proposal and listed (in *italics*) as the beginning of each task. The additional measurements were made with a view to ensuring the success of the flight tests and will thus be reported interspersed among the flight test tasks.

4.1 Task 1 – Sensor Integration

The goal of Task 1 was to build a 3-axis induction sensor and a single-axis reference sensor. These sensors were to be mounted on the boom of Sky Research's Helimag system; the following subtasks were proposed.

1. *Modify the existing design for a 3-axis induction sensor.*
2. *Select mounting locations on the boom for both sensors.*
3. *Design a mechanical structure for mounting 3-axis sensor, the amplifier, and power supply onto the boom.*
4. *Mount the sensors onto the boom.*

4.1.1 Modify the existing sensor design for a 3-axis induction sensor

Four QFS 6" induction sensors were constructed with a pass band tuned for helicopter platform magnetometry. The sensors were a simple modification of an existing design. Simple calculations indicated that target signals would fall at ~ 1 Hz and above. The helicopter rotor was known to generate a signal at ~ 15 Hz. The standard 6" induction sensor has a high pass cut-off frequency at ~ 5 Hz and a low pass cut-off in the neighborhood of 10 kHz. The SERDP SEED sensors were tuned for a high pass corner at ~ 0.4 Hz and a low pass corner at ~ 15 Hz. The transfer function for the SERDP SEED sensors is plotted against the existing sensor's transfer function in Figure 1. The transfer function and noise power spectrum for all four sensors were measured in a magnetically shielded environment, shown for one axis in Figure 2. The transfer function of all sensors was measured to be nearly identical and the noise characteristic at 1 Hz was ~ 20 pT/ $\sqrt{\text{Hz}}$ for all sensors. The noise spectrum shown has a slightly odd shape out of band, due to the fact that the magnetic noise is divided by the sensor gain at each frequency.

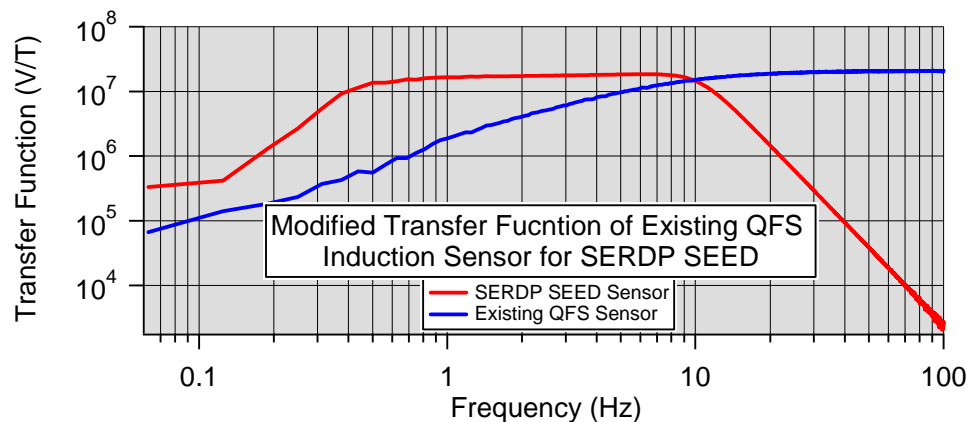


Figure 1. Comparison of existing QFS induction sensor's transfer function to that of modified SERDP SEED sensors

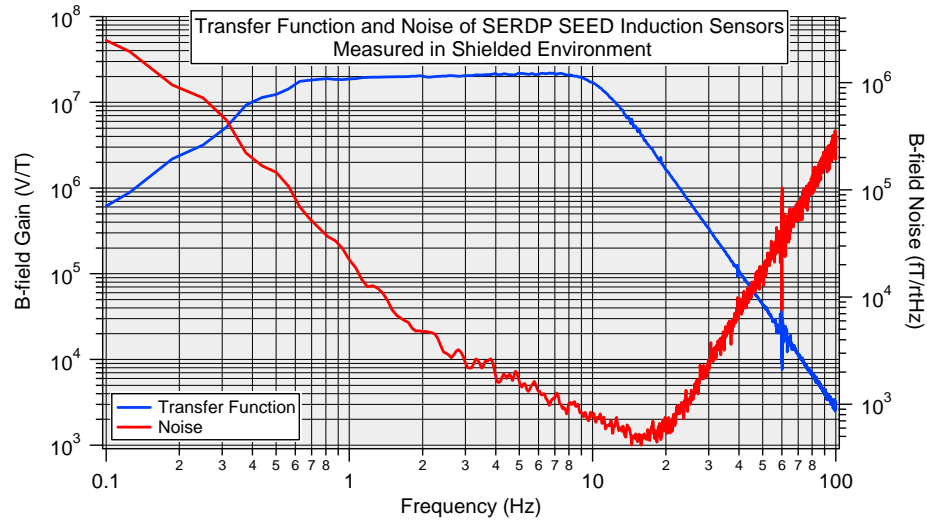


Figure 2. Transfer function and noise power spectrum of the SERDP SEED Induction Sensors referred to the sensor input (only one axis shown); pass band between ~0.4 - 15 Hz with noise floor ~ 20 pT/√Hz @ 1 Hz

Three of the inductions sensors were integrated in an orthogonal 3-axis orientation in a G-10 junction box. The preamps for the 3-axis sensor were installed in a single 3" x 4.5" x 1.5" box. The vertical (or z) axis of the 3-axis sensor, also called the main sensor, was eventually used to collect target data. The fourth sensor was to be used as the reference sensor; always aligned with the vertical axis of the 3-axis sensor. The preamp for the reference sensor was installed in its own 2.5" x 4.5" x 1.5" box. A photograph of the completed sensors and preamps is shown in Figure 3.

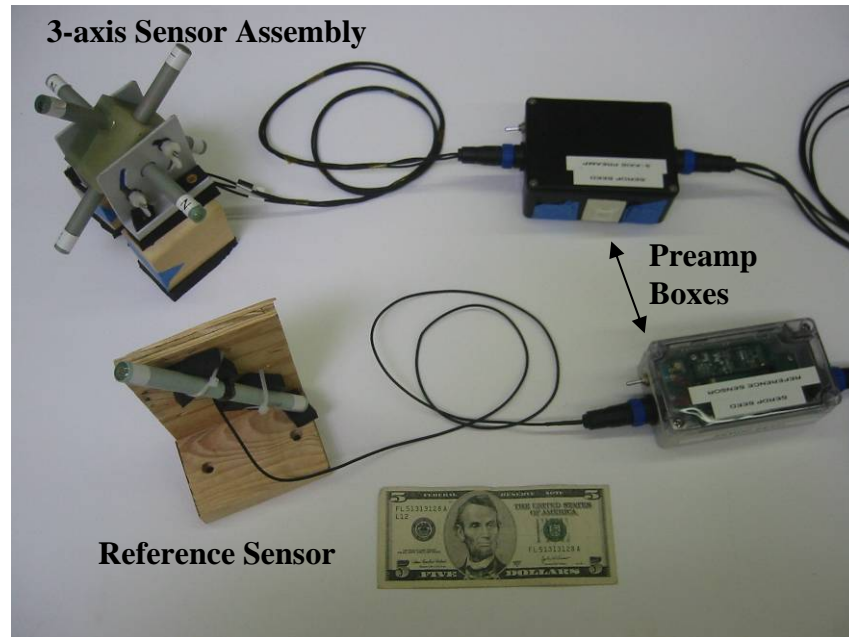


Figure 3. Photo of 3-axis sensor assembly and reference sensor, with 3-axis and single-axis preamp boxes

4.1.2 Select Mounting locations on the boom for both sensors

The Sky Research Helimag system has a Kevlar boom which extends forward ~ 4 m and has a 9 m tube running orthogonal to the center line of the helicopter; Figure 4 (left). The Helimag boom contains 7 Cs-Vapor, total-field DC magnetometers, 2 sonar sensors (to determine flight height), 2 GPS antennas, and the receiver circuitry for all these sensors. The centerline of the helicopter (next to mag sensor 4) was chosen as the mounting point for the 3-axis sensor to facilitate easy alignment of the main sensor and target during flight. The reference sensor was mounted at the right edge of the boom (next to mag sensor 7). This location was chosen so that the reference sensor would see a similar background to the main sensor, without sensing the target.

4.1.3 Design a mechanical structure for mounting 3-axis sensor, the amplifier, and power supply onto the boom

The need to align the sensors to the Earth's magnetic field meant that we needed a specific type of mounting hardware. Ideally the sensors would be mounted in a gimbal which allowed easy rotation about several axes. Sky Research had already designed and built just such a mounting structure; Figure 5 (left). The Cs-Vapor magnetometer is housed in a 2" pipe, around which the gimbal clamps. The QFS induction sensors were secured in 2" pipe flanges and mounted using the existing Sky hardware. The Sky gimbal allows two degrees of rotational freedom and can be slid back and forth through the boom (limited only by the pre-existing locations of the Sky sensors).

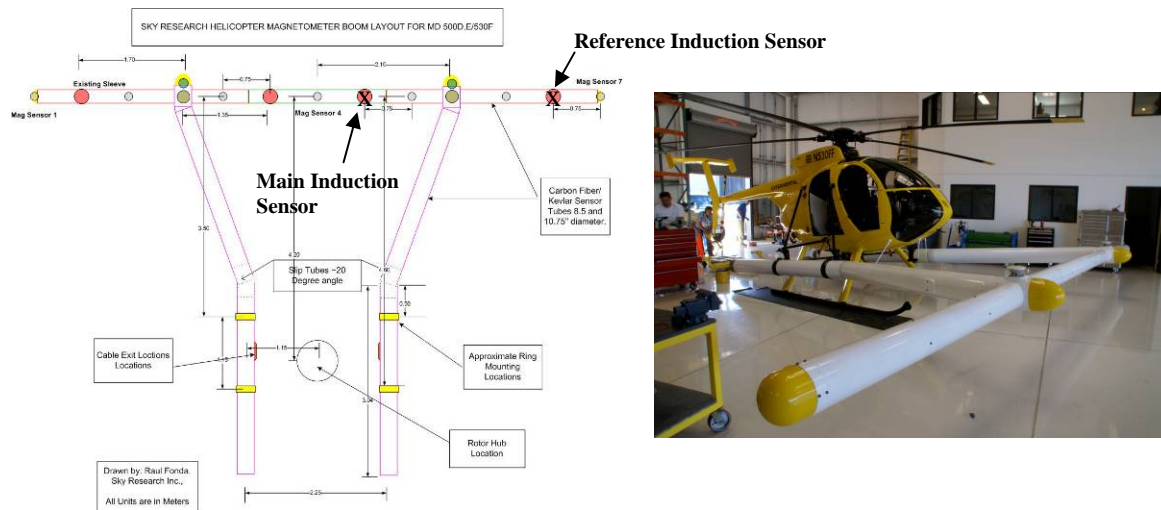


Figure 4. Left: Diagram of Sky Research's Helimag Boom. Right: Photo of assembled boom and helicopter.

4.1.4 Mount the sensors onto the boom

The sensors were mounted at the locations chosen in Subtask 1.2, using the existing Sky hardware described in Subtask 1.3. The QFS 3-axis induction sensor and the single-axis reference sensor were mounted in Sky gimbals, as pictured in below Figure 5 (middle and right). The assembled helicopter and boom (including both QFS and Sky sensors) is shown above in Fig. 4 (right).



Figure 5. Left: Photo of Sky Research sensor mounting gimbal, holding a Cs-Vapor magnetometer. Middle and Right: Sky research gimbal holding the QFS 3-axis induction sensor and single axis reference sensor.

Summary of Task 1

Four QFS 6" induction sensors were built and tuned to the desired pass band and gain. The noise characteristics of the sensors were equivalent for all four; $\sim 20 \text{ pT}/\sqrt{\text{Hz}}$ @ 1 Hz. QFS interfaced with Sky Research to select appropriate mounting positions for the sensors in the Helimag boom. QFS was able to reuse existing mounting hardware from Sky for mounting the sensors in the boom and aligning them to B_E . The sensors were rigidly mounted to the boom for the flight tests.

4.2 Task 2 – Flight Test

The goal of Task 2 was to carry out flight tests with the QFS induction sensors mounted in Sky's Helimag system. The flight tests were designed to measure the noise of the sensor during flight, and compare the signal quality with that of the Cs magnetometer.

The specific subtasks of Task 2 were as follows:

1. *Measure the sensor noise when the helicopter is on the ground, without and with the engine on*
2. *Measure the sensor noise when the helicopter is flying at 15 m/s*
3. *Determine target signatures and frequency bands of interest at two different flying heights*
4. *Perform EMI test and carry out platform noise mitigation on the ground, with the engine off and on.*

All these subtasks were completed successfully. In addition to the initially planned flight tests, QFS carried out 2 pre-flight experiments, to better anticipate the sources, strengths, and frequency bands of noise and target signals. QFS also carried out an additional experiment at the end of the program, in order to test a noise cancellation technique conceived at the conclusion of the flight tests. These experiments will be described below, interspersed chronologically with the flight tests.

4.2.1 Pre-Flight Tests

After the sensors were built and characterized, they were crudely tested in the lab. With the sensors sitting on a bench, a small munition (37 mm diameter shell, 120 mm in length) was waved nearby. In the lab, the stationary sensors could easily resolve the signal from the small shell from 1 - 2 m away. This was to be expected since the target

signal at 1 - 2 m was ~ 1 nT (at ~ 1 Hz) and the noise floor of the stationary sensors was ~ 50 pT/ $\sqrt{\text{Hz}}$ @ 1 Hz. While it was promising that the sensors could resolve the target at such a distance, this preliminary experiment did not address the problem of detection with moving sensors. In the case of moving sensors, the noise would be much higher while the target signal would remain roughly the same (with perhaps a different frequency band, depending on speed and height). There was also the possibility that motion-induced noise could saturate the sensor's preamps. Hoping to evaluate some of these issues, several pre-flight experiments were conducted to test the sensors in motion.

4.2.1a Sliding Track Experiment

The first pre-flight test was a motion track lash up. A simple 3-m sliding track was built with a sensor mount. The sensor could be slid across the track, with or without a target in the vicinity. A diagram of the slide track set-up is shown below in Figure 6 (left). Also shown in Fig. 6 (right) are the targets used in the pre-flight experiments; left target is a 57 mm shell, 170 mm tall and right target is a 37 mm shell, 120 mm tall.

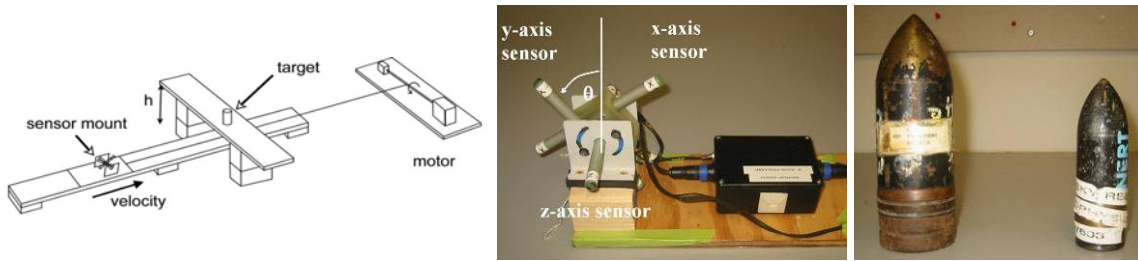


Figure 6. Left: Diagram of sliding track experiment. Center: Sliding “cart” for track; allows sensor rotation for B_E alignment. Right: Targets used for pre-flight tests, 57 mm shell and 37 mm shell left to right

The results of the sliding track experiment were promising and informative. The motion-induced noise did not saturate the sensors and detection of the 57 mm shell at close distance was possible. However the motion-induced noise was quite high. The major source of the noise was slight rotation of the induction sensors in the Earth's magnetic field. The magnetic field measured (B_m) by a vector magnetometer (such as the IS) is given by:

$$B_m = B_E [\cos \theta_o (\cos \Omega - 1) + \sin \theta_o \sin \Omega] \quad (1)$$

where B_E is the Earth's magnetic field, θ_o is the sensor's alignment to B_E , and Ω is a small perturbation about that alignment². Equation 1 above informs the reduction of noise for such sensors. Assuming small perturbations for Ω , such that $\sin \Omega$ and $\cos \Omega$ are Ω and $(1 - \Omega^2/2)$ respectively, it is evident that setting $\theta_o = 0$ minimizes B_m ; i.e.

$$B_m \cong B_E * \frac{\Omega^2}{2}; \quad \theta_o = 0; \Omega \ll 1 \quad (2)$$

In light of Eqn. 2, the track measurements were modified such that the main sensor (vertical or z axis of 3-axis sensor) was rotated down from vertical to align with B_E . In these track experiments, alignment to B_E resulted in a 17 dB reduction in noise in the band of 1-5 Hz. A further improvement, of ~ 6 dB was gained by adding vibration

damping foam at all mounting points. The results of this study are plotted in Figure 7 below. A photo of the sliding “cart”, allowing rotation of the sensor and including damping foam, is shown above in Fig. 6 (center). The plots shown are RPSD’s of the sensor noise for a vertically aligned sensor, a B_E aligned sensor, and a B_E aligned sensor with copious amounts of damping foam. Also shown is the sensor noise floor measured in the shield. NB: The noise floors after the pass band ($f > 20$ Hz) are mismatched due to gain differences in the measurements.

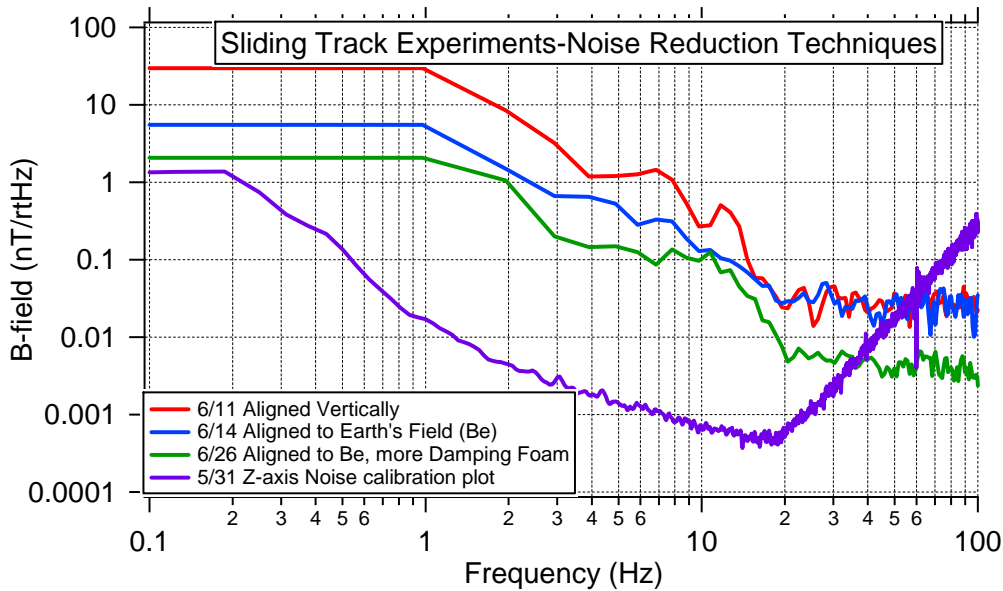


Figure 7. RPSD’s of induction sensor noise for several conditions. Alignment to Earth’s field gives ~ 10x lower noise than undamped vertical sensor.

The B_E alignment and damping foam managed to lower the sliding track noise to ~ 1 nT/ $\sqrt{\text{Hz}}$ @ 1 Hz. With this noise characteristic, target data were collected with the moving sensors. Time-domain data sets for moving sensors are shown below in Figure 8, with a simple background subtraction made. These data are taken with a 57 mm shell, located at depths = 46, 53, and 60 cm (measured from center of sensor to furthest point of target) and velocity = 0.47 m/s. The target response is clear in the data, and falls off quickly with distance; as expected for the $1/r^3$ dependence (discussed below).

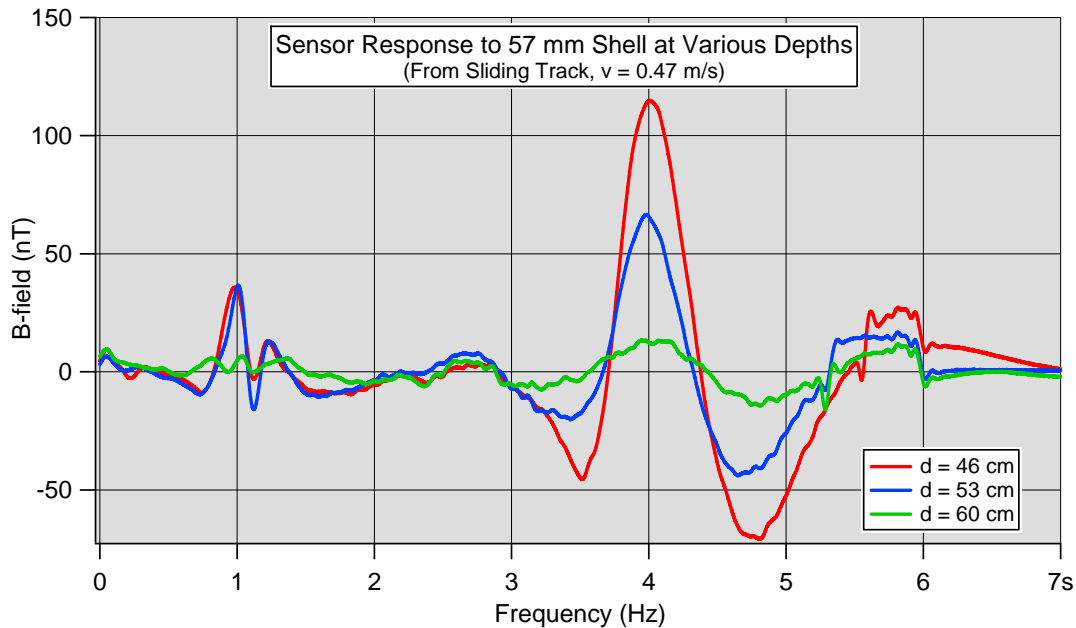


Figure 8. Time domain target responses to 57 mm shell at various heights, from sliding track experiment; $v = 0.47$ m/s.

Overall the sliding track tests were useful. The sensors did not saturate while in motion, detection was possible, and a simple noise reduction method was developed. However these track tests warranted further pre-flight experiments. The sensors measured large motional signals during periods of acceleration and deceleration (data not shown). The 3-m track was not sufficiently long enough to space the target signals (in the middle) from the acceleration/deceleration signals (at the ends). Furthermore, the sliding track experiments were carried out far from other metal objects and were still too close to a lab set-up. Hence the second pre-flight test was carried out: ground vehicle tests.

4.2.1b Ground Vehicle Tests

The sliding tracks tests were successful, but did not allow enough acquisition time for the target signals to be adequately spaced between acceleration and deceleration signals at the ends of the data sets. Furthermore it was desirable to mount the sensors on a large metal object which would move in the sensor's frame; more closely approximating a helicopter. Thus the second pre-flight test was to mount the sensors on a vehicle and drive past targets.

A simple boom was made from wood, extending out from either side of the vehicle (a light pickup truck). For ease of mounting, the 3-axis sensor needed to be flipped such that the Y-axis served as the main sensor (for this test only). The main sensor and the reference sensor were aligned to the Earth's magnetic field, shown in Figure 9. Data were collected for the vehicle moving on a dirt road in one direction (east-west) to ensure alignment of the sensors to B_E .



Figure 9. Photos of vehicle tests. Left: Boom with 3-axis sensor mounted on driver's side and reference sensor mounted on passenger side. Right: Close-up of 3-axis sensor mounted on boom and aligned to Earth's field.

In an effort to eliminate the acceleration noise in the beginning of the acquisition, the vehicle first began moving; and once a constant velocity of 10 mph was reached, the DAQ began acquiring data. A time-domain data set from the vehicle test is shown below in Figure 10. The 57 mm shell is at depth = 32 cm, measured from the center of the sensor to the bottom of the target. The target signal is clear in the data at $t \sim 12$ s and the high noise associated with deceleration can be seen at $t > 14$ s. Note: The Y-axis was used as the main sensor in these tests.

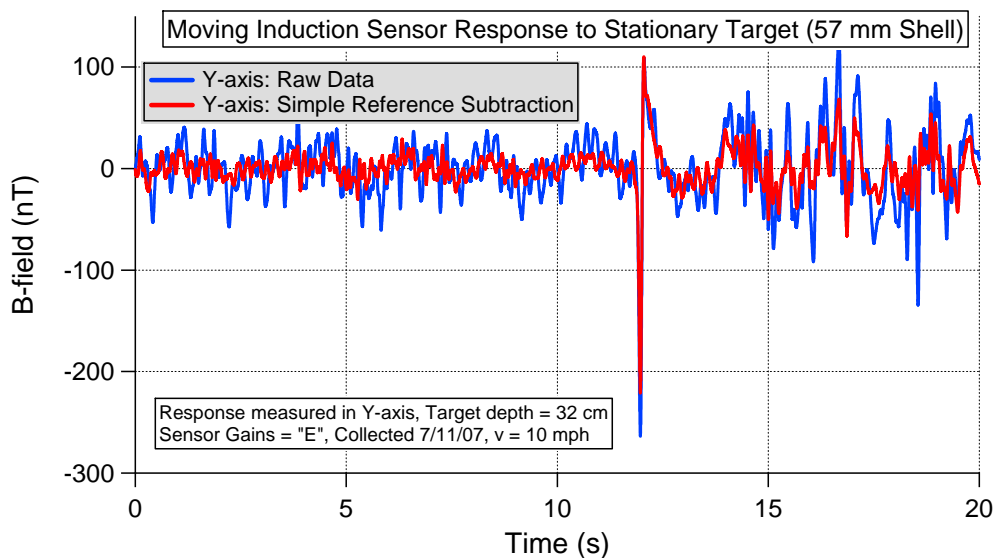


Figure 10. Time-domain data from sensors mounted on vehicle; response to 57 mm shell at 32 cm. Shown with reference sensor background subtraction.

The vehicle test was another success. Once again the sensors did not saturate and the target signal was very clear. A simple background subtraction was made using the reference sensor. The time-domain data show a fairly regular background pattern, mainly comprised of two frequencies; a slow ~ 0.25 Hz signal probably due to motion-induced sensor rotation and a ~ 2 Hz signal probably from the spinning magnetic moment of the vehicle's wheels. The reference sensor improved the SNR by 2x, from ~ 3.5 to ~ 7 , by

cancelling the coherent noise from the wheels (at 2 Hz) but did not prove very effective at cancelling the slow rotational noise. This was attributed to inadequate coherence of motion-induced noise between the main and reference sensors. It was thought that the helicopter boom and the mounting scheme for the sensor in the boom would improve this situation.

4.2.2 Flight Tests

A test plan was submitted to the SERDP office by QFS³ and approved prior to the tests. The flight tests were carried out according to the test plan at Sky's headquarters in Ashland, OR during the week of September 24th, 2007.

The test site was a grass field running roughly North-South between the taxi-way and runway of a small airfield. The length of the test field was ~ 3600 m. Sky Research's hangar and test facility is located just off the airfield. The flight plan was discussed with the Sky Team, who said the helicopter could comfortably fly at heights above 1.5 m and at velocities between 5 – 30 m/s.

The QFS sensors were mounted near Sky sensors 4 and 7 (main and reference sensor respectively) with induction sensor preamps resting inside the boom and the output signals routed to a 16-bit National Instruments DAQ system running on a Laptop in the cockpit. The main (vertical or z) axis of the 3-axis sensor was aligned to the Earth's field, as was the reference sensor. The sensor's orientations were locked in place in the Sky mounting gimbals. With this set-up, the flight tests commenced.

4.2.2.1 Measure the sensor noise when the helicopter is on the ground, without and with the engine on

Before the sensors were mounted, they were set up in the middle of the airfield for a background noise data collection. The stationary environmental background had very low noise in the sensor band. The sensors were subsequently mounted in the boom for other noise data collections.

As outlined in the flight plan, noise data were collected for incrementally noisier steps:

1. helicopter on tarmac, not running
2. helicopter on tarmac, blades running
3. helicopter on grass, blades running
4. helicopter flying at high altitude $h \sim 100$ m, $v \sim 5$ m/s
5. helicopter flying over clear field $h \sim 1.5$ m, $v \sim 10$ m/s

These data were all analyzed in post processing to evaluate the noise floor of the sensors while flying. The noise power spectra for these experiments are shown in Figure 11, along with the shielded noise floor of the sensors. The shielded noise floor of the sensor is ~ 20 pT/ $\sqrt{\text{Hz}}$ @ 1 Hz (black). The vibrations from the running helicopter blades raise the noise floor to ~ 500 pT/ $\sqrt{\text{Hz}}$ @ 1 Hz (orange). The helicopter flying at $h = 1.5$ m, $v = 10$ m/s gives a noise characteristic of ~ 10 nT/ $\sqrt{\text{Hz}}$ @ 1 Hz (blue); roughly 500x over the sensor noise floor. The motion-induced noise from flying appears broadband, between 0.1 and 3 Hz. The data also show distinct peaks at slightly higher frequency, 5 - 8 Hz;

probably caused by the helicopter's rotor. These peaks are easy to eliminate in post processing, being regular and well defined signals. In light of the low target signal band, future sensors could be tuned for a lower pass band, such that they reject signals above 5 Hz.

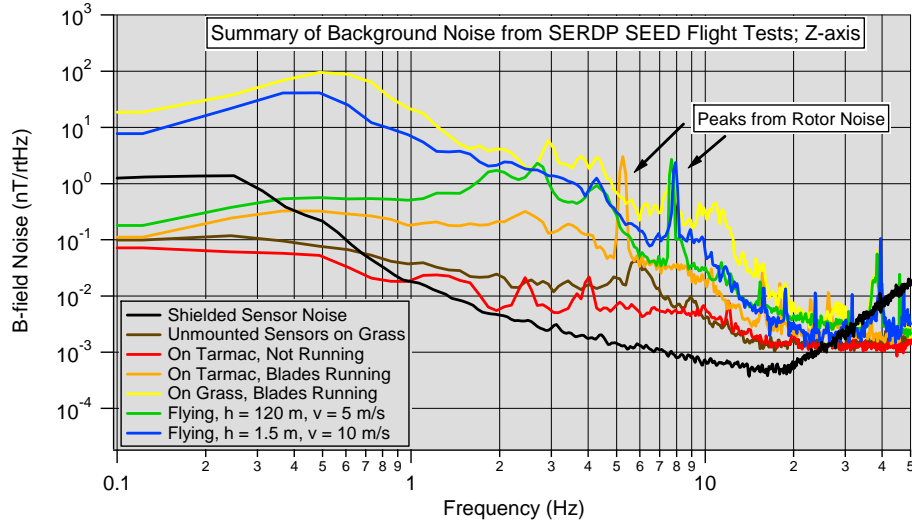


Figure 11. Noise power spectra for various conditions during the flight tests. Typical flight noise in induction sensor is ~ 500x higher than sensor noise floor @ 1 Hz; 10 nT/√Hz compared to 20 pT/√Hz.

An estimate of the degree of rotation at a given frequency can be made from Fig. 11 and using a simplified version of Eqn. 1. Taking the vector projection of B_E onto the sensor, B_m , to be $B_m = B_E \cos(\theta_0)$, and assuming the sensor is then rotated through a small angle Ω due to the motion of the platform, gives

$$B_m = B_E [\cos(\theta_0) - \cos(\theta_0 + \Omega)] \quad (3)$$

Equation 3 can then be differentiated to give the measured magnetic field through rotation,

$$dB_m = B_E \sin(\theta_0) d\Omega \quad (4)$$

where $d\Omega$ is now a rotation characteristic. At 1 Hz Fig. 11, shows a B-field noise of ~ 10 nT/√Hz for the sensor in flight. Using this value for dB_m , and assuming an alignment error to the Earth's field of $\theta_0 = 10^\circ$, then the rotation spectrum at this frequency is 0.07 deg/√Hz. This estimate is confirmed by the off-axis data (in this case, x-axis) for which an angle of $\theta_0 = 80^\circ$ can be assumed (data not shown).

It is possible that some of the rotational noise could be actively cancelled in future systems by measuring the rotation of the sensor with a gyroscope. The resolution of such a gyroscope would have to be high enough to measure the magnetic field induced in the sensor by small rotations. There are commercially available gyroscopes which can provide this sensitivity. Applied Technology Associates, for example, have developed a gyroscope (the ARS-01) with < 80 μradians of noise over the band of 1-1000 Hz; which roughly equates to 3 μrad/√Hz. This rotational resolution can be converted to a rotational magnetic noise resolution using Eqn. 4. Plugging in 3 μrad/√Hz for $d\Omega$ in Eqn. 4, and

assuming an angle of $\theta_0 = 10^\circ$, gives a magnetic noise resolution $26 \text{ pT}/\sqrt{\text{Hz}}$ @ 1 Hz, much lower than the target IS noise characteristic of $100 \text{ pT}/\sqrt{\text{Hz}}$ @ 1 Hz. For an alignment angle of $\theta_0 = 45^\circ$ (for the sensor need not ever be more than 45° off from B_E), the resolution becomes $106 \text{ pT}/\sqrt{\text{Hz}}$ @ 1 Hz. Thus this gyroscope could be employed to cancel rotational noise even if the sensor is not aligned with B_E . The effectiveness of this method may be efficient enough to allow the use of vertical and horizontal sensors, thus eliminating the need for B_E alignment.

4.2.2.2 Measure the sensor noise when the helicopter is flying at different speeds

In addition to the noise tests described above, the helicopter was flown at several speeds for a fixed height. It seemed likely that there would be an optimal speed where rotation and vibration were both minimized, while target signal was maximized. Vibration in the helicopter is chiefly induced through the rotating blades, and thus higher velocity means more vibration. Rotation has the opposite effect; at low velocities the helicopter experiences ground effects and has a tendency to pitch and roll. As velocity is increased, the flight becomes more stable and there is much less rotational noise. The target response is maximized in the flat region of the sensor's transfer function; namely between ~ 0.4 and ~ 15 Hz (discussed below). If the flight height and velocity place the target signal below 0.4 Hz, flying faster can give more target signal. The noise power spectra for three flights at the height of 1.5 m are plotted below in Figure 12. The flight at $v = 10 \text{ m/s}$ seems marginally better over most of the pass band.

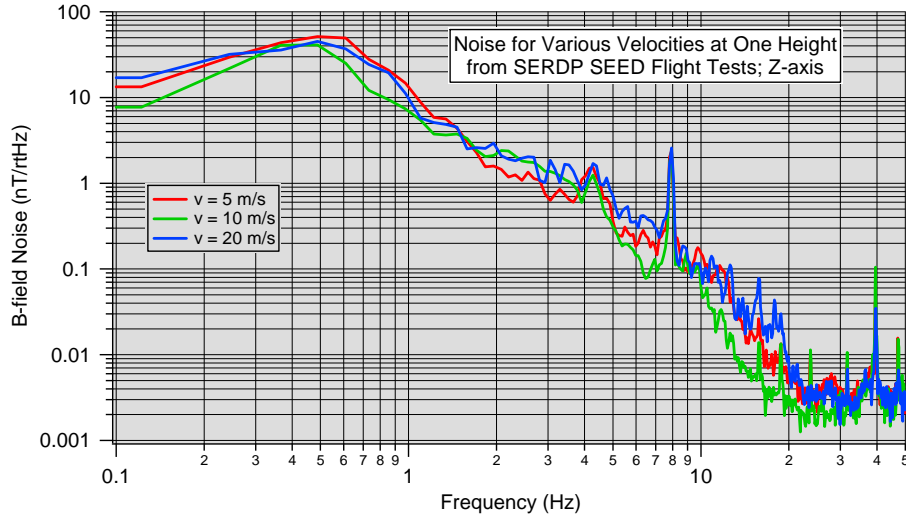


Figure 12. Noise power spectra of three flights of different velocity and same height. The flight at $v = 10 \text{ m/s}$ seems marginally better across the pass band.

4.2.2.3 Determine target signatures and frequency bands of interest at two different flying heights

The frequency band of the target signal is fairly simple to model. The magnetic field of a magnetically permeable object in the Earth's field is an induced dipole. The magnetic field from a dipole is given by

$$\vec{B}(r) = \frac{\mu_o}{4\pi r^3} \vec{m} \times \vec{r} \quad (5)$$

where μ_0 is the magnetic permeability of free space, m is the magnetic dipole moment, and r is the distance between source and field point. Thus a sensor moving along the horizontal “x-direction” and passing over a target senses a vertical B-field $B_z(x)$. Taking the Δx as the full width at half max (FWHM) of $B_z(x)$ and dividing Δx by the platform velocity gives the time ΔT over which the sensor sees the target. Thus the frequency of the target signal can be approximated by using $f = 1/\Delta T$. A more sophisticated approach is to calculate $B_z(x)$ over some range of x larger than that in which the target is seen, divide by velocity to convert to a time domain signal, and take a Rapid Power Spectrum Density (RPSD) of that simulated time-domain data. Taking the FWHM of this RPSD will yield the frequency band for that particular target.

Prior to the flight tests, a simple model was developed based on the principle outlined above. The model was made in LabVIEW and allowed user entry of m , v , and h . The model calculated the vertical and horizontal B-field for a vertical target on the ground, sensed by a magnetometer aligned to some other angle (say, along the Earth’s field). A screen shot of the latest version of this program is shown in Figure 13 below. Thus the signal frequency band and amplitude can be calculated at various heights, velocities, or magnetic moments. Subtask 2.3 calls for the frequency band at two heights. Using a magnetic moment of $0.85 \text{ A}\cdot\text{m}^2$ (probable for a large UXO target) and a velocity of 10 m/s , the target signal and signal band is calculated for 1.5 m and 3 m .

- The band of interest for $h = 1.5 \text{ m}$ is $0.6\text{-}3 \text{ Hz}$
- The band of interest for $h = 3 \text{ m}$ is $0.3\text{-}1.8 \text{ Hz}$

Thus the chosen pass band for the induction sensors is appropriate. It is important to note that the target frequency band, namely $\sim 0.5 - 3 \text{ Hz}$, is roughly the same as the band of rotational noise plotted in Fig. 11.

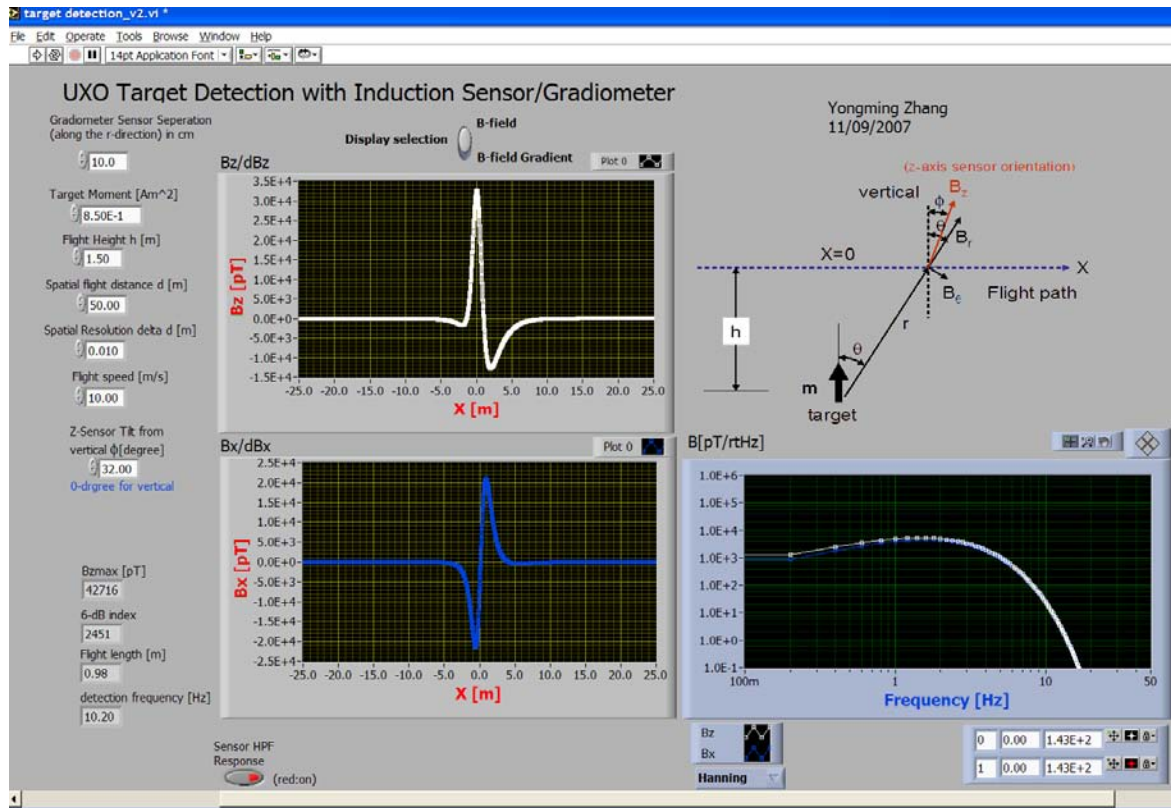


Figure 13. Screen shot of LabVIEW based model of B-field from UXO for given height, velocity, and moment.

In addition to the model, target data were collected during the flight tests. The target runs utilized Sky Research's standard calibration test set. The test set consisted of 2 each of 4 different objects: (1) a 100 lb bomb simulant, (2) a 155 mm shell, (3) a 2.75" rocket tip, and (4) an 8" steel cube; shown and labeled in Figure 14 (left). Seven targets were laid along the test lane, spaced 40 m apart, in the following configuration:

- 100 lb bomb simulant-vertical
- 155 mm rocket-vertical
- 2.75" rocket-vertical
- 8" cube
- 100 lb bomb simulant-horizontal- +45° from parallel
- 155 mm rocket- horizontal- +45° from parallel
- 2.75" rocket- horizontal- +45° from parallel (note: this target was placed 80 m from second to last target due to asphalt lane crossing test lane)

The helicopter flew at heights 1.5 and 3 m, at speeds ranging from 5 – 30 m/s; Fig. 14 (right). In general the $h = 1.5$ m, $v = 20$ m/s flights showed the best performance, largely due to noise limitations (discussed below). Although the 10 m/s flights had shown slightly lower noise, 20 m/s yielded more target signal by moving the frequency into the flat region of the sensor's transfer function.

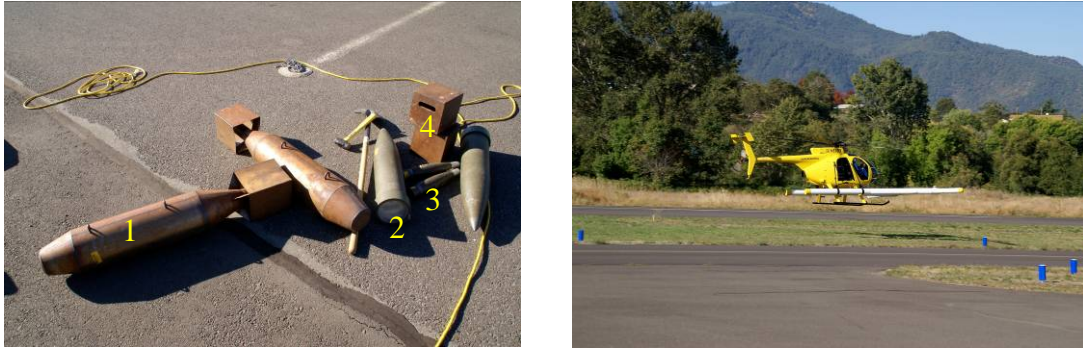


Figure 14. Left: Sky Research's standard calibration test set of targets, labeled 1, 2, 3, and 4. Right: Helimag system flying along test lane at $h = 1.5$ m, $v = 20$ m/s.

4.2.2.4 Perform EMI test and carry out platform noise mitigation on the ground, with the engine off and on

The pre-flight experiments and the target signal model informed the data collection during the flight tests. The initial stationary data collection in the test field indicated that the sensor gain setting was appropriate. The main and reference sensors were aligned to the Earth's field and mounted with vibration damping foam. In pre-flight tests, the reference sensor showed good potential for coherent noise cancellation. The sensor pass bands were matched to the target signal band.

In addition to all these counter measures for noise, a 3-axis accelerometer was installed along side the sensor. The hope for the accelerometer was that it might provide information about rotation and vibration that could be used to cancel motion-induced noise in the sensor.

As the flight tests progressed, it became clear that the reference sensor was not coherent with the main sensor. This incoherence was largely due to torsion modes in the helicopter boom and the presence of large metal objects near the runway. In short, the reference sensor did not see the same magnetic background, minus the target, as the main sensor. No change was made to the sensor configuration after the initial set-up. Alterations to the boom/sensor assembly seemed prohibitively time consuming for the limited test time available. Instead the hope was to use the off-axis sensors (i.e. x and y) in the 3-axis assembly to cancel the motional noise. The benefit of a 3-axis sensor over a single main sensor is the added target and noise information gained. The x and y axis are rigidly mounted with the z-axis, and thus the motion induced noise is coherent between all 3. Using Eqn. 1, the motion-induced noise in z could be cancelled using data from x and y.

As mentioned, the best target detection performance was found in the $h = 1.5$ m, $v = 20$ m/s target test flights. The frequency band of both the target signal and the motional noise are roughly the same and the signal levels have similar amplitudes. The raw data from the best of the 1.5 m, 20 m/s target runs are shown in Figure 15(top). The target signal from the 100 lb bomb can be seen as spikes in the data at $t \sim 12$ and 18 s. The other targets are hard to discriminate in these data.

The data plotted in Fig. 15 (middle) show the same data set, but after it had been processed with the help of the Sky Research team. The data were put through a mean filter, in which a smoothed average of the data set (essentially most of the noise with little of the signal) is subtracted from the raw data, and some low pass filtering is applied. The characteristic of the raw data, from Fig. 11, is $\sim 10 \text{ nT}/\sqrt{\text{Hz}}$ @ 1 Hz. With mean filtering, this figure is lowered to $\sim 2 \text{ nT}/\sqrt{\text{Hz}}$ @ 1 Hz (data not shown).

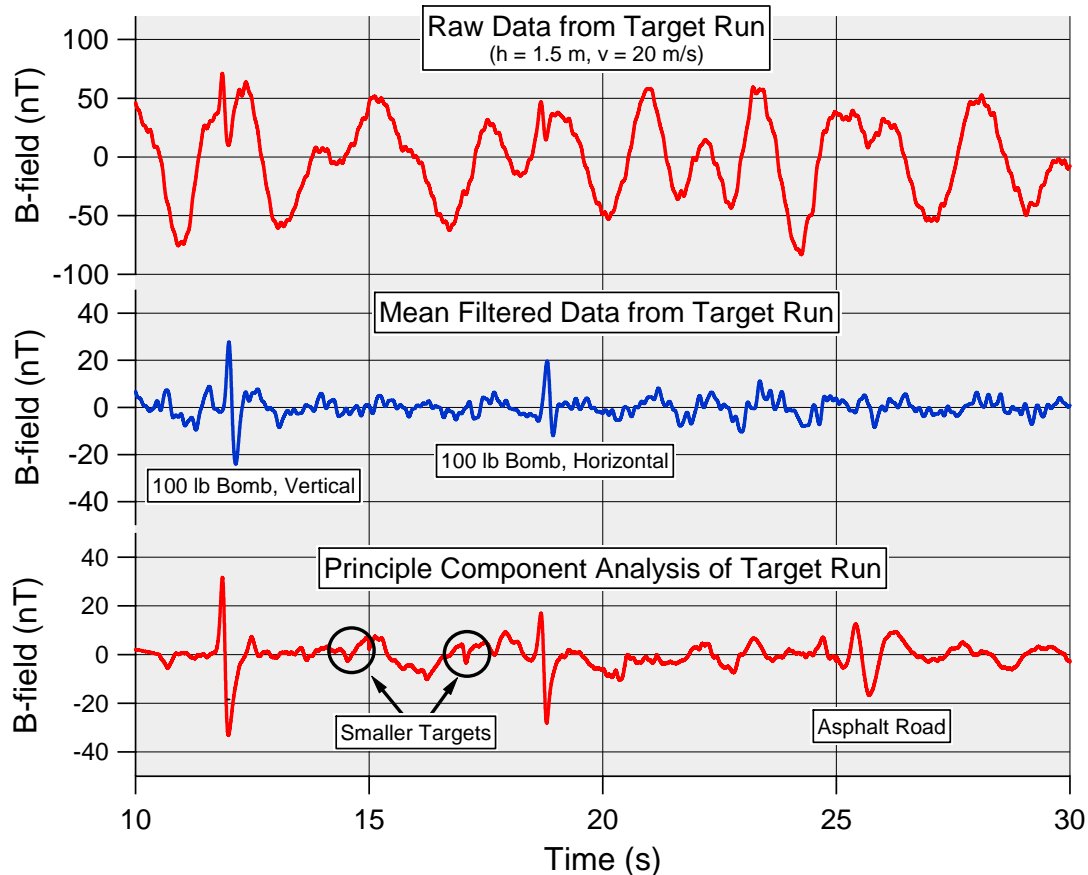


Figure 15. Best case data from flight test target runs. Top: Raw data. Middle: Mean filtered data; 100 lb bomb can be seen at $t \sim 12 \text{ s}$ and $t \sim 18 \text{ s}$. Bottom: Target run data processed with principle component analysis.

In the raw data the target signal (peak-to-peak) is 82 nT and the standard deviation of the data set is 35 nT, giving an SNR ~ 2 . The mean filtered data has target amplitude of 52 nT with data set standard deviation of 4 nT, for SNR ~ 13 . Typically an SNR of 3 is considered adequate for detection for a single data acquisition. Therefore, with processing, the QFS induction sensors can detect at least the larger targets.

A further analysis of the data was conducted at QFS using principal component analysis. Principal component analysis is a method of looking at multi-channel data for signals that are present in more than one channel by examining the correlations between the channels. The correlated signals can then be removed, leaving signals that are primarily present in

only the channel of interest. In this case, the motion artifact needs to be canceled, and data from all channels were used; 3-axis sensor, reference sensor, and accelerometer.

This analysis found little coherence between the reference and main channels, and zero coherence between the 3-axis sensor and accelerometer. This is due to the fact that the accelerometer measures linear acceleration and not actual sensor rotation or orientation during the flight, while the sensor magnetic noise was caused by rotation of the sensor in the Earth's field. A rotation sensor should be utilized, instead of the linear accelerometer. However the off-axis channels from the 3-axis sensor (i.e. x and y) did prove useful in this analysis. The bottom plot of Fig. 15 shows the same data set processed with principal component analysis. The signal amplitude of the first target is 64 nT and the data standard deviation is 5.5 nT, giving an $\text{SNR} = 11.6$. In this plot the smaller targets can just start to be seen amidst the noise.

The data from Sky Research's Cs-Vapor magnetometer 4 (located next to QFS main sensor) over the same target run are shown in Figure 16. The data were passed through a mean filter and a 5 Hz low pass filter. A processed noise of ~ 1 nT is evident. The Cs-vapor magnetometer easily sees the 100 lb bomb simulants, with $\text{SNR} \sim 20\text{-}30$. Most of the smaller targets (the 2.75" rocket-horizontal is not seen) can be seen in the data, with SNR's of $\sim 2\text{-}5$.

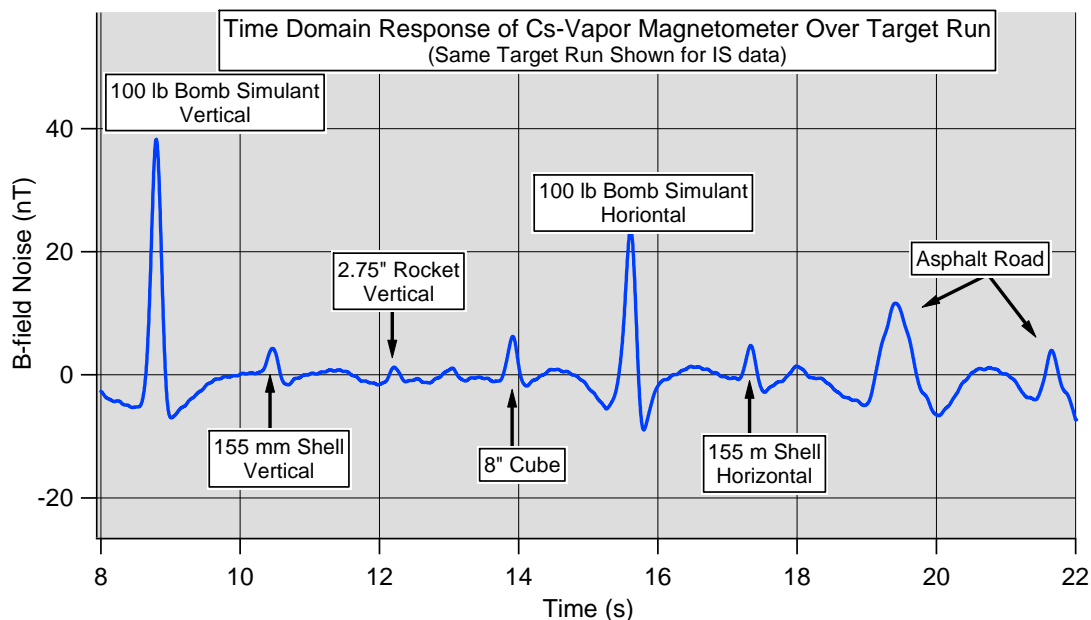


Figure 16. Plot of Sky Research's Cs-vapor magnetometer data (processed), over the same target run. The Cs-vapor sensors have a processed noise floor of ~ 1 nT.

4.2.3 Post-Flight Tests

Following the flight test and subsequent data analysis, it became clear that the reference sensor was not being utilized properly. The off-axes in the 3-axis sensor gave some noise cancellation, but the ideal case would be a sensor measuring the exact same background as the main sensor, without sensing the target signal. The conclusion made was that a reference sensor mounted rigidly and directly above the main sensor would measure the

same motion-induced noise. The reference sensor would only measure a tiny portion of the B-field signal from the target, since the target signal has a $1/r^3$ dependence (Eqn. 5). This configuration of magnetometers is called a gradiometer.

Thus the 3-axis induction sensor and the reference sensor were mounted together vertically to form a gradiometer in that direction, using a rigid tube to hold them in place. The vehicle tests of the pre-flight tests were repeated for this new gradiometer configuration. Photos of the gradiometer set-up and vehicle test are shown in Figure 17.



Figure 17. Left: Gradiometer configuration with reference sensor mounted rigidly above 3-axis main sensor. Right: Repeat of vehicle tests with gradiometer, using 57 mm shell target.

The procedure of the second (gradiometer) vehicle tests was largely the same as the first. The sensors were mounted on a wooden boom hanging out from the vehicle (a light pickup truck). The vehicle traveled West-East and the sensors were aligned to the Earth's magnetic field. Magnetometer data were collected from both the main and the reference sensor and the subtraction (to produce gradiometer data) was done in post processing. This configuration allowed a direct comparison of an IS magnetometer to an IS gradiometer. A comparison was also made of vertically aligned sensors to Earth's field aligned sensors, shown in Figure 18. The results were as follows:

- A factor of 2.5x noise reduction is seen in going from vertically aligned sensors to B_E aligned sensors, which is similar to the flight data.
- The magnetometer aligned to B_E shows a similar noise performance to the magnetometer in the flight tests, $\sim 20 \text{ nT}/\sqrt{\text{Hz}}$ @ 1 Hz.
- A factor of $\sim 10x$ noise reduction is seen in going from B_E aligned magnetometer to B_E aligned gradiometer.
- Altogether a factor of $\sim 25x$ noise reduction is achieved in going from a vertical magnetometer to a B_E aligned gradiometer.

The measurement implies that an IS gradiometer could easily achieve an in-flight noise floor of $1\text{-}2 \text{ nT}/\sqrt{\text{Hz}}$ @ 1 Hz. A carefully constructed gradiometer, with finely tuned relative alignment, pick-up, and phase would achieve an even greater noise reduction. Additionally, a 3-axis gradiometer would allow the off-axis noise cancellation used

above. Thus an IS gradiometer could potentially achieve an in-flight noise floor of $< 100 \text{ pT}/\sqrt{\text{Hz}}$ @ 1 Hz or lower.

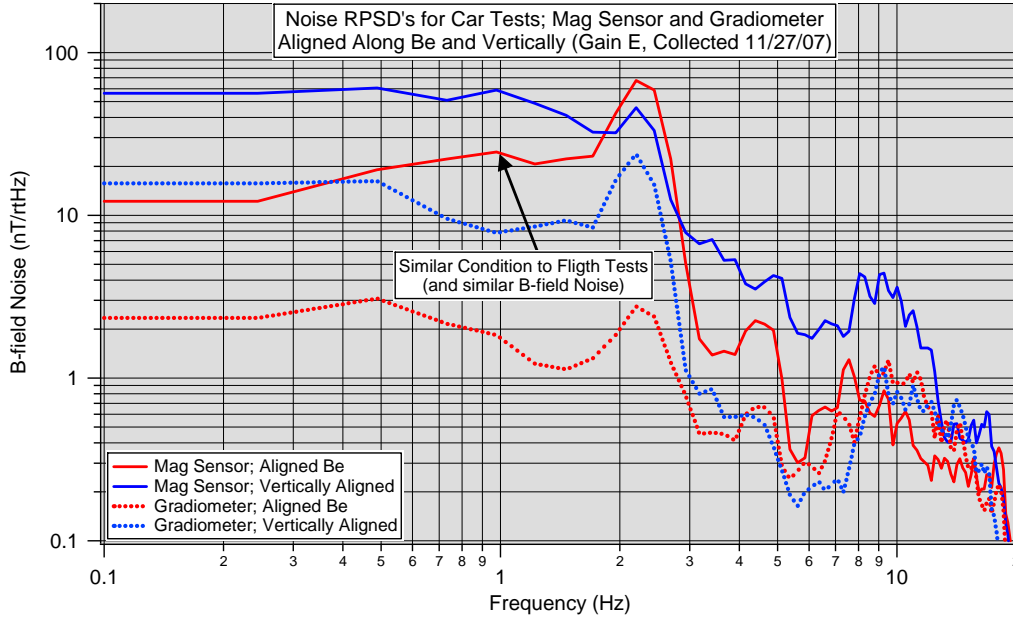


Figure 18. Noise power spectra for IS magnetometer vs. IS gradiometer, aligned vertically and to B_E . IS magnetometer aligned to B_E shows similar noise performance to flight tests (@ 1 Hz). IS gradiometer aligned to B_E has ~ 25x lower noise than vertical IS magnetometer and ~ 10x lower noise than B_E aligned IS magnetometer.

As in the original vehicle tests, target data were collected using the 57 mm shell, plotted in Figure 19. The shell was placed at a depth of 53 cm (center of gradiometer to bottom of shell) and the vehicle was traveling 10 mph. The red plot shows the raw magnetometer data and the blue plot shows the gradiometer data, calculated by:

$$B_{grad} = B_{main} - k * B_{ref} \quad (6)$$

where k is some scale factor, found by comparing the relative RPSD amplitudes at the strongest frequency (in this case 1.925 Hz). The magnetometer data show a peak-to-peak signal amplitude of 474 nT and a variance of 63 nT; SNR = 7.5. The gradiometer data have signal amplitude 253 nT and a variance of 10 nT; SNR = 25. Thus the crude gradiometer shows an SNR improvement of $> 3x$. This improvement would almost certainly be greater for a more carefully constructed gradiometer and more heavily processed data.

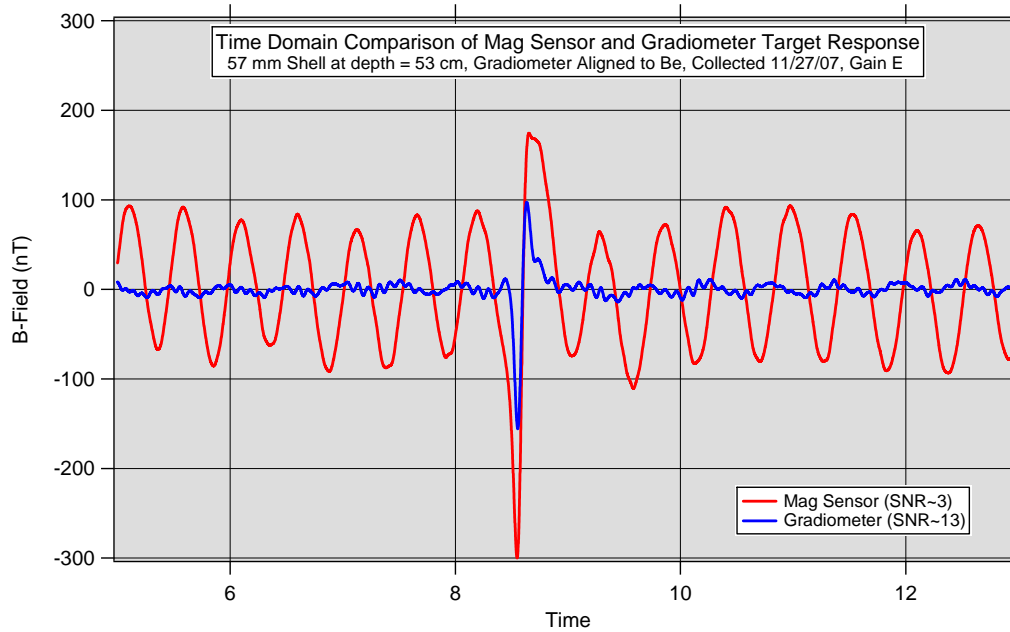


Figure 19. Time-domain target response of B_E aligned magnetometer and gradiometer. An SNR improvement of > 3 is gained by the gradiometer

A low noise induction sensor gradiometer could be constructed in a package slightly larger than the current induction sensors. The induction sensors used in this program were 6" long with a noise floor of $\sim 20 \text{ pT}/\sqrt{\text{Hz}}$ @ 1 Hz. This noise floor is easily pushed down to $10 \text{ pT}/\sqrt{\text{Hz}}$ @ 1 Hz (the typical 6" IS noise spec.). A 6.5" IS gradiometer could be built with two 2.25" induction sensors and 2" of sensor separation. The noise floor of the IS's is proportional to the square of the length; a 2.25" IS would have $\sim 7x$ more noise, or a noise characteristic of $\sim 80 \text{ pT}/\sqrt{\text{Hz}}$ @ 1 Hz. Thus a 6.5" IS gradiometer could be built from two 2.25" IS, having a noise floor of $\sim 80 \text{ pT}/\sqrt{\text{Hz}}$ @ 1 Hz. This IS gradiometer would fit in the helicopter boom and would have a noise floor lower than the desired detection noise floor of $100 \text{ pT}/\sqrt{\text{Hz}}$ @ 1 Hz.

Summary of Task 2

QFS carried out two pre-flight experiments to better anticipate the noise and signals that would appear during the flight test. A moving track experiment was constructed and the sensors were mounted on a vehicle moving over the targets. These tests indicated that the IS needed to be aligned to the Earth's magnetic field to reduce motion-induced noise in the vector sensors. The reference sensor showed good potential for coherent noise cancellation.

The flight plan was submitted to SERDP and carried out as planned. Noise power spectra were collected with the sensors in a variety of stationary and moving tests. The noise characteristic during a typical flight was $\sim 10 \text{ nT}/\sqrt{\text{Hz}}$ @ 1 Hz, $\sim 500x$ higher than the sensor noise floor. An SNR of ~ 2 was measured for large targets (100 lb bomb simulant) at flight height = 1.5 m, which could be improved to ~ 13 with mean filtering. The reference sensor did not have sufficient coherence with the main sensor to provide any noise cancellation; however the off-axis sensors in the 3-axis sensor assembly were able

to cancel some motion-induced noise through principal component analysis; giving an SNR of ~ 12 .

After the flight tests, a new mounting configuration was tested for the reference sensors. The reference sensor was mounted rigidly and directly above the main sensor in a gradiometer configuration. The vehicle tests were repeated with the gradiometer. The induction sensor magnetometer performance was compared to that of an induction sensor gradiometer, for cases of vertical and B_E alignment. The B_E aligned IS magnetometer has the same noise performance in the post-flight vehicle tests as it did during the flight tests. The B_E aligned gradiometer showed at least 10x lower noise than the B_E aligned magnetometer. It is therefore reasonable to assume that the flight noise characteristic could be lowered by $\sim 10x$. *Thus the IS gradiometer would achieve in-flight noise levels of about $1 \text{ nT}/\sqrt{\text{Hz}}$ @ 1 Hz .* A more carefully constructed gradiometer, a more sophisticated noise mitigation/analysis scheme, and the use of a 3-axis gradiometer would likely improve this noise performance further, down to $\text{sub-nT}/\sqrt{\text{Hz}}$ @ 1 Hz .

4.3 Task 3 – Reporting and Management

The flight test plan called for a comparison table between QFS's IS and the Cs-Vapor magnetometer. The goal was that the IS should meet or exceed the performance of the total field magnetometers. The sensor comparison is detailed below in Table 1.

Table 1. Performance assessment metric to evaluate QFS I.S. performance.

Metric	Description	Qualitative/ Quantitative	Observed results
Ease of use	<i>Complexity of set up/ reliability</i>	<i>qualitative</i>	The QFS sensors were mounted in the existing Sky gimbals. Set-up complexity was equivalent for both sensors. Both sensors functioned 100% of the test, with equivalent reliability. QFS sensors score over Cs-Vapor sensors by being lighter and smaller ; 1.8 oz and 0.439” diameter compared to 2 lbs and 2” diameter.
Flight envelope restrictions	<i>Survey altitude/stability</i>	<i>quantitative</i>	The QFS sensors in the test limited the flight envelope to one direction by requiring alignment to Earth’s field, whereas the Cs magnetometers allow bidirectional flight. Use of a three-axis IS gradiometer would allow bidirectional flight, making the flight envelope identical to Cs mags.
Target SNR	<i>SNR as determined for test targets</i>	<i>quantitative</i>	Compare SNR for 100 lb bomb. The Cs mags have ~ 10x better SNR than the QFS IS’s, by having 10x lower noise (1 nT compared to 10 nT). The use of an IS gradiometer would meet and possibly exceed noise (and SNR) performance of the Cs mags.
Target Location	<i>Derived locations of UXO targets</i>	<i>quantitative</i>	In cases of adequate SNR, location of targets is equivalent between IS and Cs magnetometers. The use of a 3-axis vector sensors still holds the potential to give better discrimination of the target; i.e. location, shape, and orientation.

QFS filed 3 quarterly reports for the program. A flight test plan was submitted to the SERDP and accepted with revisions.

Sky Research helped coordinate the flight tests and oversaw the operation of the Helimag system during the test. Sky aided with the IS data analysis from the flight test, as well as provided Cs-Vapor magnetometer data for the final report.

QFS and Sky agreed that the flight test was a successfully executed test plan as well as a successful collaboration for both parties. Figure 20 shows the Sky and QFS teams at the completion of the test.



Figure 20. Sky Research and QFS teams at the completion of flight tests, photographed at Sky Research headquarters in Ashland, OR; taken 9/27/07

5. Technical Feasibility and Conclusions

The key lessons of this SEED feasibility study are as follows:

- The target signals involved in airborne UXO detection are in the frequency band of 0.5 - 3 Hz, with field strengths of $\sim 1 - 80$ nT.
- The major source of noise for a moving induction sensor is rotation in the Earth's magnetic field. This noise is broadband over a 0.5 – 3 Hz range, with field strengths of 10 – 80 nT.
- A 6"-long induction sensor vertically aligned has an in-flight noise characteristic of $60 \text{ nT}/\sqrt{\text{Hz}}$ @ 1 Hz; 60 times greater than a Cs-vapor magnetometer and 3,000 times greater than the sensor noise floor.
- Motion-induced noise in an induction sensor is reduced by aligning the sensor to the Earth's magnetic field. A B_E aligned induction sensor has an in-flight noise characteristic of $10 \text{ nT}/\sqrt{\text{Hz}}$ @ 1 Hz.
- With processing, a B_E aligned induction sensor can achieve an in-flight noise characteristic of $2 \text{ nT}/\sqrt{\text{Hz}}$ @ 1 Hz and an SNR as high as 13 for a 100 lb bomb stimulant, which is more than adequate for detection of large targets. This sensor has trouble resolving smaller targets due to high levels of motion-induced noise.

The key success of the program is as follows:

A quick prototype induction sensor gradiometer was able to achieve a simulated flight (vehicle-based) noise characteristic of about $1 \text{ nT}/\sqrt{\text{Hz}}$ @ 1 Hz. This noise figure could potentially be much lower through one or more of the following improvements: a more carefully constructed gradiometer, a 3-axis sensor, a more sophisticated data analysis/noise cancellation scheme, or a commercial rotation sensor (i.e. a gyroscope). QFS believes a noise characteristic of $100 \text{ pT}/\sqrt{\text{Hz}}$ @ 1 Hz is feasible.

QFS believes that the induction sensor gradiometer holds great promise for airborne UXO detection. A 3-axis IS gradiometer would score over the Cs-vapor magnetometer in several regards:

1. It can be made more sensitive; allowing detection from greater heights or of smaller targets.
2. It is a vector sensor which will enable not only target detection, but also target discrimination by providing information about the target shape and orientation.
3. Use of a 3-axis IS gradiometer would allow bidirectional flight, thus eliminating flight envelope restrictions.
4. The IS gradiometer can be made much lighter and smaller; 6.5" long, 0.5" diameter, < 2 oz in weight. Currently Sky Research must employ 150 lbs of ballast in the rear of the helicopter to offset the weight of all the sensors and receiver electronics in the front of the boom. Reducing the sensor weight (and thus, the ballast) is highly desirable for safety and flight efficiency.

6. Recommendations for Next Phase

Collaborating with Sky Research, QFS plans to propose a 2-year SERDP program to develop and demonstrate a 3-axis gradiometer for the Helimag platform. The basic program tasks, by year, would be:

Year 1: Develop the 3-axis gradiometer. The main tasks will be:

- Build 3 carefully matched and rigidly mounted induction sensor gradiometers and mount together in a 3-axis assembly
- Optimize sensor separation distance and total sensor length
- Carry out multiple flight tests, perform noise measurement and target detection, and to characterize and optimize the sensor
- Investigate potential noise reduction through use of a commercial gyroscope (to measure rotation parameters)
- Study noise cancellation with off-axis sensors
- Develop noise cancellation algorithms and processing scheme.

Year 2: Demonstrate functionality and detection ability

- Build multiple sensors (possibly 7) to replace Cs-vapor sensors in Helimag system
- Carry out multiple flight tests with multi-sensor array
- Characterize and discriminate standard target signals
- Compare results with the Cs-vapor based Airborne System

7. References

¹ Foley, JE, "Helicopter Magnetometry Characterization: Integrated Technology for Wide Area Assessment," 2005 SERDP/ESTCP Symposium

² Robert J. Dinger and John R. Davis, Proceedings of the IEEE, Vol. 64, No. 10, October 1976, pgs. 1504-1511

³ "Helicopter Magnetometer Platform based on Compact Induction Sensors-Flight Test Plan", Submitted to SERDP office, (SERDP SEED Project 1594:2006), Version Sept 7, 2007